Cristelo N et al., Influence of fibre reinforcement on the post-cracking behaviour of a cement-stabilised sandy-clay subjected to indirect tensile stress, *Construction and Building Materials, Elsevier*, 138: 163-173, 2017.
Doi: 10.1016/j.conbuildmat.2017.02.010

January 2017

Influence of fibre reinforcement on the post-cracking behaviour of a cement-stabilised Sandy-Clay subjected to indirect tensile stress

[a,*] Nuno Cristelo; [b] Vítor M.C.F. Cunha; [c] António Topa Gomes; [b] Nuno Araújo; [b] Tiago Miranda; [c] Maria de Lurdes Lopes

[a] CQVR, Department of Engineering, University of Trás-os-Montes e Alto Douro, 5001-801 Vila Real, Portugal
[*] Corresponding author
Telephone: + 351 259 350 388; Telefax: + 351 259 350 356
E-mail address: ncristel@utad.pt

[b] ISISE, Department of Civil Engineering, University of Minho, 4800-058 Guimarães, Portugal

[c] Construct, Faculty of Engineering, University of Porto, 4200-465 Porto, Portugal

Abstract

An experimental campaign was carried out to determine the influence of polypropylene fibre content and length on the post-cracking response of a Sandy-Clay stabilised with different cement contents. Three main sets of specimens were prepared: cement-stabilised specimens with two cement contents (5% and 10%); fibre-reinforced specimens with three fibre contents (0.1%, 0.2% and 0.3%) and cement-fibre-reinforced specimens combining the mentioned fibre and cement contents. Tensile tests on the fibres and indirect tensile tests and triaxial compression tests on the prepared specimens were conducted. Results show that the post-cracking behaviour is strongly affected by the combination of fibre and cement content as well as fibre length. Pull-out was the governing failure mode. Post-peak tension loss rate increased with fibre content, as a result of the loss of influence of the fibres on the post-peak behaviour. On the contrary, an increase in fibre content resulted in higher pre-peak strength gain rates and higher peak stresses.

Keywords: Geosynthetics; Soil improvement; Fibre reinforcement; Residual tensile strength; Cement stabilisation

Doi: 10.1016/j.conbuildmat.2017.02.010

1. Introduction

Even though fibre reinforcement has been attracting the attention of the geotechnical community for some time, the technique has recently gained a renewed interest and is now the subject of several research works. This renewed enthusiasm is based on promising research and application results, which show that the technique is quite effective and might be a good solution for geotechnical structures in which the settlements (serviceability aspects) do not have a huge impact on its design criteria, such as earth embankments, backfill of both gravity and reinforced retaining walls (Eldesouky et al., 2013) and slope stabilisation (Gregory and Chill, 1998; Gregory, 2011a, 2011b, 1998), or even more settlement-dependent geotechnical structures, like strip footings (Nasr, 2014).

It is well known that the addition of discrete fibres to a brittle matrix can provide different types of benefits, based on the additional resistance to crack initiation and, mainly, on the crack width restraint and residual strength enhancement. Within the geotechnical context, distinct studies have also been conducted to assess the benefits of reinforcing soils with randomly distributed discrete fibres on the soil's mechanical properties, namely on the uniaxial and triaxial compression and direct shear behaviour (Al-Refeai, 1991; Cai et al., 2006; Chauhan et al., 2008; Consoli et al., 2010; Cristelo et al., 2015; Diambra et al., 2010; Falorca and Pinto, 2011; Hamidi and Hooresfand, 2013; Lirer et al., 2011; Michalowski and Čermák, 2003; Nasr, 2014; Tang et al., 2007, 2010; Yi et al., 2015; Yilmaz, 2015; Zhang et al., 2015; Zhu et al., 2014). Additionally, and since every type of soil has a very poor response to tensile stresses, the use of fibres to improve the soil's behaviour when subjected to such stresses is very appealing and has thus been the subject of several research papers (Correia et al., 2015; Li et al., 2014; Olgun, 2013). However, the simultaneous use of cement and discrete fibre reinforcement creates a complex material in terms of tensile strength, especially on the post-peak stress segment of the load-displacement curve. This structural response has not yet been fully characterised, and is thus the main subject of the present paper.

In general, the fibres are responsible for an increase of the compressive and shear strength, especially at the post-peak and residual (post-cracking) stages, and the extent of such improvement is intrinsically dependent of several factors, such as: fibre properties, geometry and content; fibre distribution and orientation within the matrix; existence and magnitude of artificial cementation (using, for instance, Portland cement or lime); and fibre-soil bonding (stress-slip behaviour).

The present paper aims a thorough characterisation of the tensile stress post-peak response of a polypropylene fibre reinforced sandy-clay. It is part of an extensive research programme designed to understand the mechanical response of a very common Portuguese soil, when reinforced with fibres, as well as the potential need for additional chemical stabilisation. The experimental work comprised indirect tensile splitting tests of sandy-clay soil specimens with and without discrete fibre reinforcement (0.1, 0.2 and 0.3% by dry weight), and with or without Portland cement (5.0 and 10.0% by dry weight), tensile stress tests on the fibres and triaxial tests on the reinforced soil, to assess the confined constitutive behaviour.

2. Experimental program

2.1. Materials characterisation

Additional geotechnical and microstructural details, as well as a more thorough explanation on the preparation of the fibres, can be found in (Cristelo et al., 2015). The following is the essential information presented in the aforementioned paper.

The soil was collected in the Campus of the University of Trás-os-Montes e Alto Douro (UTAD), in the northeast of Portugal. Geotechnical characterisation is summarised in Table 1, and based on these the soil was classified as CL – Sandy Lean Clay (ASTM D2487, 2011).

Table 1
Main geotechnical properties of the soil, including particle size distribution

Property		Value	Unit
Plastic Limit		14.59	%
Liquid Limit		23.46	%
Organic matter content		2.64	%
Soil particle density		26.83	kN/m^3
D_{50}		0.045	mm
Uniformity Coefficient		6.92	-
Curvature Coefficient		0.53	-
Optim. water content [a]		13.5	%
Max. dry unit weight [a]		18.9	kN/m^3
Size (mm)	Passing (%)	Size (mm)	Passing (%)
9.51	98.36	0.075	55.58
4.76	96.07	0.043	48.64
2.00	92.64	0.031	40.16
0.841	86.52	0.021	23.19
0.425	81.34	0.013	11.88
0.250	77.63	0.009	6.22
0.180	70.22	0.006	3.39
0.106	65.03	0.003	0.57

[a] Standard Proctor test

Microstructural characterisation of the soil, using scanning electron microscope (SEM) and X-ray energy dispersive spectrometry (EDS) analysis, revealed that almost 80% of the soil is constituted by silica and alumina, while the use of cement significantly increased the calcium content of the original soil. X-Ray diffraction patterns of the soil showed the presence of quartz, calcite, illite, nacrite and muscovite on the mineralogical composition (Cristelo et al., 2015).

Portland cement CEM I-42.5R (where R stands for initial high strength cement, with a minimum compressive strength of 20 and 42.5 MPa, respectively, at 2 and 28 days, according to NP EN 197-1 standard) and polypropylene (C_3H_6) fibres were used. According to the manufacturers' specifications, the density of the fibres and the cement was 8.92 kN/m^3 and 30.89 kN/m^3, respectively. The fibres had an average diameter of 31 μm and length of approximately 12 and 49 mm. Also according to the manufacture's specifications, these fibres have characteristic tensile stress and ultimate strain of 220 MPa and 111.1 %, respectively. In order to confirm these values, and due to the importance of the fibres' tensile stress-strain response for the present study, a set of tensile tests was performed in order to validate the information obtained from the manufacture.

2.2. Specimen fabrication

Preparation of the soil included drying and de-flocculation by hand. Soil-cement specimens were dry mixed for 10 min in a Hobart counter mixer, and two different cement/soil weight ratios of 0.05/0.95 (5%) and 0.10/0.90 (10%) were used. The fibres were then carefully added, by hand, in weight ratios of 0.001, 0.002 and 0.003, and an additional 10 min mixing period was followed. The water (deionised) was the last component to be added, prompting an additional 10 min mixing period. The fibres were considered as part of the solids, instead of part of the voids' volume (Ibraim et al., 2012). The overall microstructure of a soil-cement-fibre mixture is generally depicted in Figure 1, in which it is possible to observe the relative dimensions between the soil particles and the fibres.

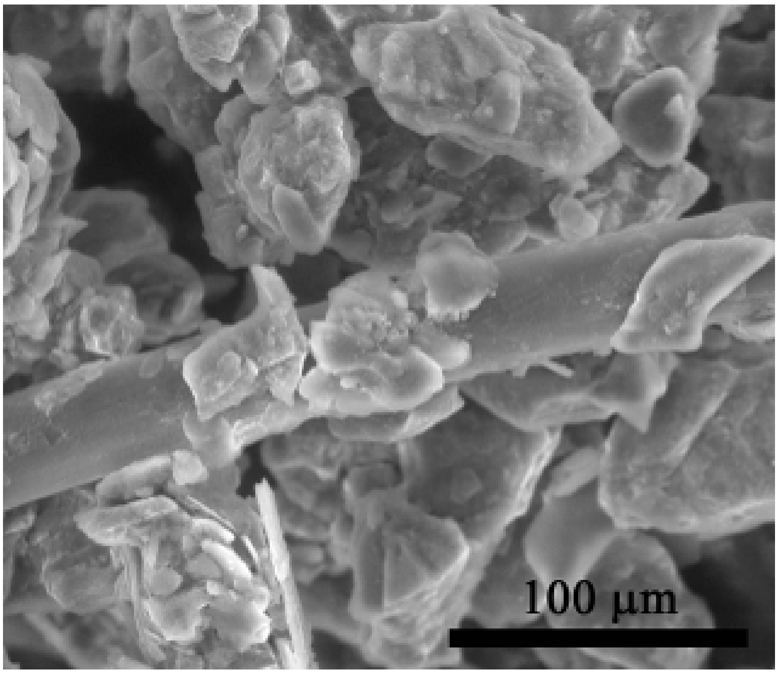

Figure 1: Microstructural spatial arrangement of the soil particles and the fibres

All the specimens were moulded with a dry unit weight of 18.0 kN/m^3 (as mentioned, the fibres' mass was included as part of the solids' mass). A water content of 16% was used to fabricate every specimen, independently of the inclusion of cement and/or fibres. Both the dry density and the water content do not match the ideal compaction characteristics, with values below and above the maximum dry density and optimum water content, respectively. The reason for this water excess was to account for the cement hydration, and the corresponding reduction in dry density was needed to keep the moulding point on the Proctor test curve. The voids ratio of each type of mixture (identified in Table 2) was calculated based on the density of each material (soil, cement and fibres) and their respective weight proportions. Forty-eight hours after compaction, during which the top and bottom of the moulds were covered with cling film and kept at 20ºC ± 1º and 90% RH ± 3%, the specimens were demoulded and left to cure, in the same previous conditions, for the remaining of the 28 days period.

Table 2
Identification and characterisation of all the mixtures fabricated

Label	Fibre [a,b] content (%)	Cement content (%)	Fibre length (mm)	w/c	Voids [b] ratio
TA.0.0	0.0	0.0	-	-	0.491
TA.1.0	0.0	5.0	-	3.200	0.502
TA.2.0	0.0	10.0	-	1.600	0.513
TB.0.1	0.1	0.0	12.9	-	0.490
TB.1.1	0.1	5.0	12.9	3.197	0.501
TB.2.1	0.1	10.0	12.9	1.598	0.512
TB.0.2	0.1	0.0	49.54	-	0.490
TB.1.2	0.1	5.0	49.54	3.197	0.501
TB.2.2	0.1	10.0	49.54	1.598	0.512
TC.0.1	0.2	0.0	12.9	-	0.489
TC.1.1	0.2	5.0	12.9	3.195	0.500
TC.2.1	0.2	10.0	12.9	1.598	0.511
TC.0.2	0.2	0.0	49.54	-	0.489
TC.1.2	0.2	5.0	49.54	3.195	0.500
TC.2.2	0.2	10.0	49.54	1.598	0.511
TD.0.1	0.3	0.0	12.9	-	0.488
TD.1.1	0.3	5.0	12.9	3.192	0.499
TD.2.1	0.3	10.0	12.9	1.596	0.510
TD.0.2	0.3	0.0	49.54	-	0.488
TD.1.2	0.3	5.0	49.54	3.192	0.499
TD.2.2	0.3	10.0	49.54	1.596	0.510

[a] Relatively to the soil + cement weight

[b] Considering the fibres as part of the solids content

The cylindrical specimens used in the indirect tensile tests (IT) were compacted in three equal layers, using static compaction, with a diameter of 70 mm and height of 140 mm. Four different types of specimens were prepared for the triaxial tests (TC): unreinforced specimens (previously designated by TA.0.0), cement-reinforced specimens (TA.2.0), fibre-reinforced specimens (TC.0.2) and cement-fibre-reinforced specimens (TC.2.2). The TC specimens were fabricated with the same properties of the IT specimens' (i.e. void ratio, dry unit weight and water content) and diameter (70 mm). However, due to the need to accommodate the axial strain sensors (linear displacement transducers), the height of the TC specimens was 160 mm, instead of the 140 mm used for the IT specimens.

2.3. Tensile testing of the fibres

Due to the difficulties associated with the tensile test of a single fibre – regarding the gripping setup necessary to apply the tensile force and also the extremely low tensile strength of one single fibre, which proved to be impossible to read accurately using the available load cell – it was decided to test several fibres simultaneously, with each set composed by 10 fibres. For that purpose, two plastic tubes, with a diameter of 5 mm, were used to hold both ends of each of the 10 fibres (Figure 2). The fibres were held in place while one of the tubes was filled with glue. After this first end was dry, the second end of the fibres was inserted in the other tube and kept stretched while the glue was applied. That way it was possible to guarantee that the 10 fibres had precisely the same free length between both tubes, which was then accurately measured. This procedure made possible to firmly restrain the ends of the 10 fibre set in the metallic grips (Figure 3). An Instron® Microtensile Tester, model 5848, with a 2 kN load capacity, was then used to perform the tests and to obtain the full stress-strain curves. Each specimen had a gauge length of 25 mm, and the tests were carried out under displacement control, with an extension rate of 0.2 mm/min. Every test was stopped only after all the fibres had failed, since no slipping between the fibres and the gripping system was detected. The room temperature during the tests was recorded at 22.5ºC ± 0.5ºC.

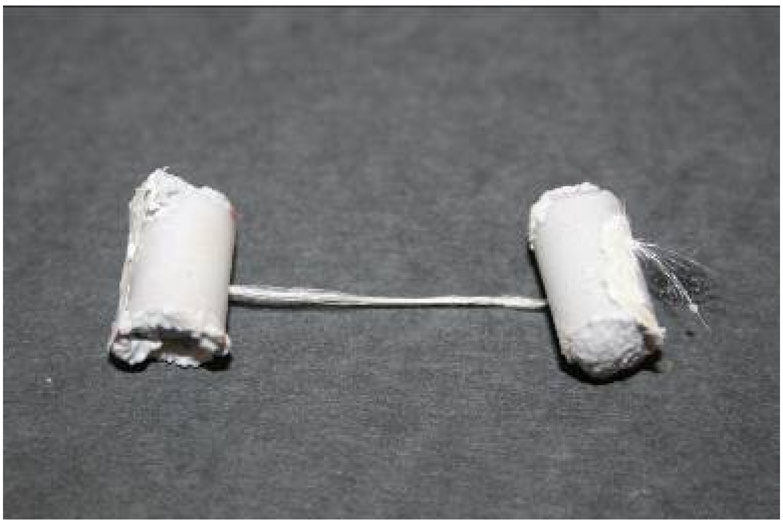

Figure 2: Set of 10 fibres used for the tensile tests

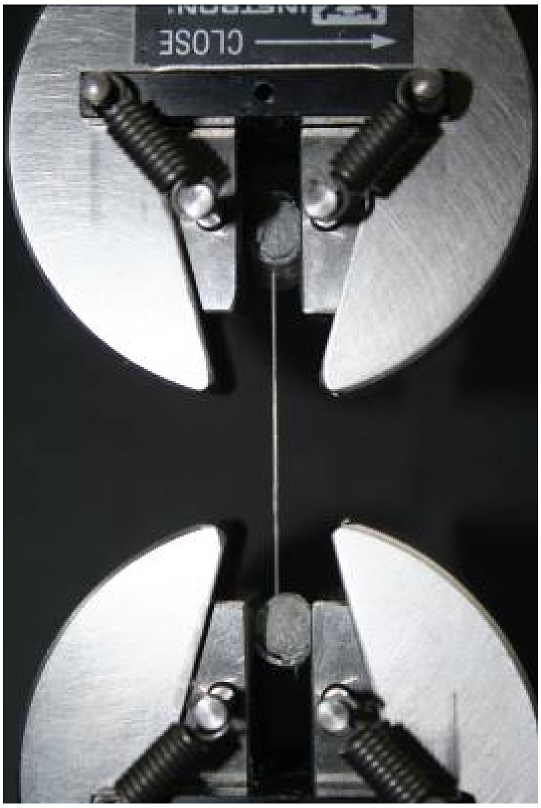

Figure 3: Initial phase of a tensile test, showing the ends of the fibres' set firmly restrained by the grips

2.4. Indirect tensile testing

An Instron® electro-mechanical testing rig, fitted with a 10 kN load cell, was used for the indirect tensile strength tests. The tests were carried out under monotonic displacement control, at a rate of 0.4 mm/min, and the entire stress-strain curve was obtained from each test. Three specimens per mixture were prepared and tested. Based on British Standards recommendations (BSi EN 13286, 2003), two prismatic hardboard packing strips, with dimensions 140x7x4 mm^3, were installed on opposite generatrices of the specimen (Figure 4). Each strip was discarded after only one application. The relative displacement of the loading plates was taken as the average readings of two LVDT sensors.

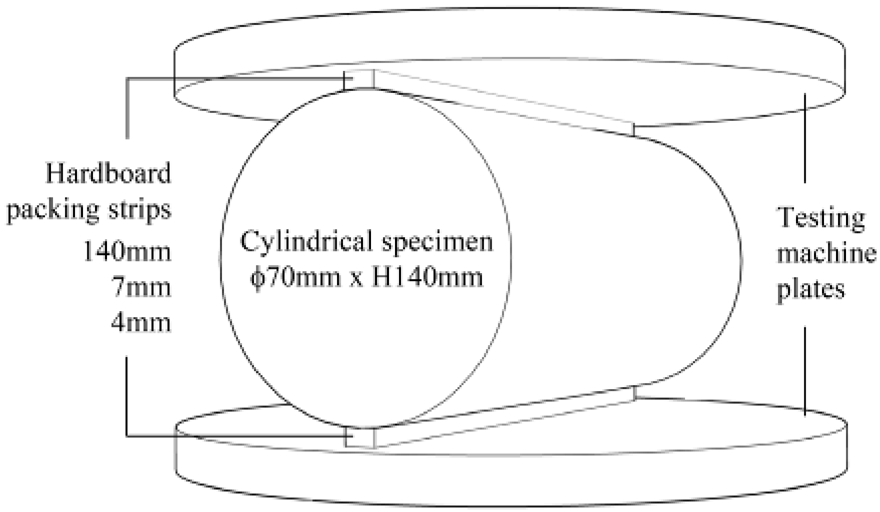

Figure 4: Indirect tensile test setup (EN 13286, 2003)

2.5. Triaxial testing

Two consolidated-drained (CD) triaxial compression tests (Figure 5) were performed per selected mixture, using consolidation isotropic effective stress states of p'=10 kPa and p'=50 kPa. A servo-hydraulic testing rig, fitted with a 25 kN load cell, was used to apply the deviatoric load, under monotonic displacement control, at a rate of 0.01 mm/min. Such relatively low displacement rate was used in order to monitor the development of any unexpected pore water pressure, since the specimen was not initially saturated (an initial assumption was made that the reduction in the unsaturated void ratio during the test would not be sufficient to develop pore water pressures). The entire stress-strain curve was obtained from each test. The specimen axial deformation was the average of the readouts of two Linear Displacement Transducers (LDT), while an additional LDT was installed to monitor the radial deformation.

Figure 5: Triaxial test setup showing Linear Displacement Transformers (LDT) instrumentation

3. Experimental results

3.1. Tensile behaviour of the fibres

The results of 5 tensile tests are presented in Figure 6. Based on these results, and considering that a total of 10 fibres were tested simultaneously, each with a diameter of 31 μm, the average maximum tensile stress and secant Young's module (at 50% of the peak stress) of 426 MPa and 2.67 GPa, respectively, were estimated. These results were based on the stress values corresponding to a strain level of 35%, and the overall evolution and absolute values of these curves are in accordance with those obtained by Ibraim et al. (2012). The design tensile stress defined by the manufacturer was approximately 50% of the average estimated tension value, which suggests a factor of safety of 2.

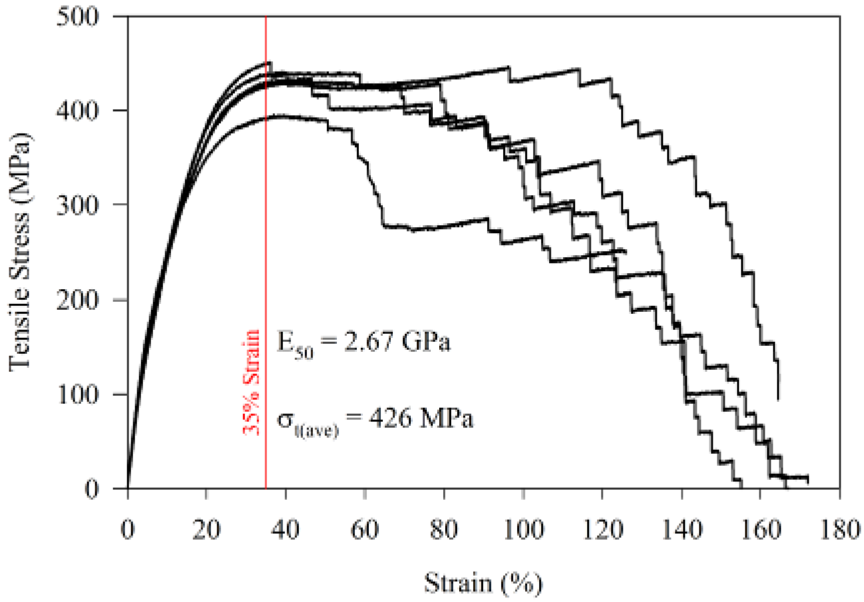

Figure 6: Tensile stress-strain curves obtained with sets of 10 fibres

3.2. Indirect tensile behaviour

The force-displacement curves obtained during the indirect tensile tests are shown in Figure 7. The effect of cement content is very clear, with the increase in cement content producing a consistent increase in both the stiffness and peak stress. This effect is confirmed by the images presented in Figure 8 – obtained as soon as the peak stress was reached – showing the increase in the crack width with the decrease of the cement content, for the series reinforced with 0.20% fibres.

Although the fibres' effect is visible in the pre-peak branch, it is more preponderant on the post-peak behaviour, with an increase in ductility (5% and 10% cement) translated by the appearance of strain-softening on the fibre reinforced mixtures, as opposed to the abrupt decline of unreinforced mixtures (0% fibres). However, it is worth noting that the post-peak strain-softening slopes of the 10% cement specimens tended to similar load levels, independently of the fibre content (0.1, 0.2 and 0.3%), and the same occurred for the 0% and 5% cement specimens. For higher diametric strains (defined as the reduction of diameter in the vertical direction divided by the initial diameter) the post-peak response appears to depend mostly on the fibre content, and less on the cement content. With the crack widening and the corresponding decline in tensile strength of the soil-cement matrix, the fibres become the only resistance to the tensile stress imposed.

Another particularly interesting nuance is the sudden decline, after the peak load, of the curves correspondent to the materials with 5% and especially 10% cement (dark circles in Figure 7). In some cases, this decline was almost immediately followed by a second phase of strength increase which, in the case of the 5% cement mixtures, reached even higher strength levels than in the original phase of strength increase. Several authors have reported such behaviour (Olgun, 2013; Sobhan and Mashnad, 2002). The development of this second phase of strength increase is related to distinct micromechanical mechanisms:

- The cement reinforced soil matrix, which has a lower tensile strength than the fibres, starts to be elastically deformed up to the formation of micro-cracks, which will then coalesce into a macro-crack roughly when the peak load is attained.
- After the localization of the inelastic deformation, the crack width increase was followed by a sudden decrease of the load, whereas the fibres become progressively mobilized, bridging the stresses along the crack surfaces and leading to a small pseudo-hardening stage. As the fibres are further mobilized, distinct fibre reinforcement mechanisms may occur depending on the fibre and cement content, as well as fibre

length. In general, for the mixtures with the lower cement content, the smooth softening post-peak behaviour may indicate that the fibres were fully pulled out, which was confirmed by visual examination. On the contrary, for the highest cement content mixtures, the main failure mechanism was fibre rupture (based also on visual examination) possibly due to a higher interface bond strength.

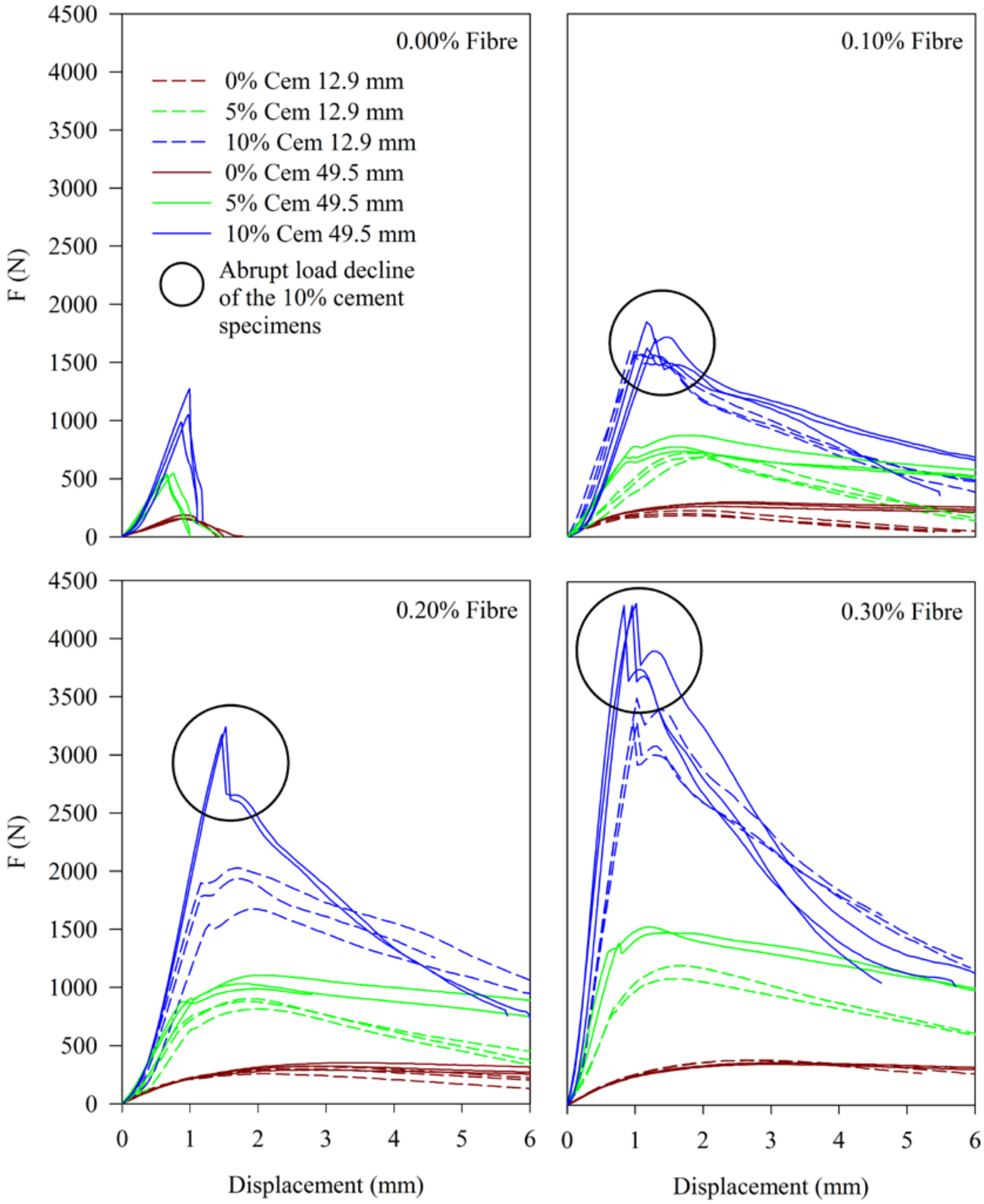

Figure 7: Force-displacement curves, as a function of the fibre content, obtained during the indirect tensile strength tests

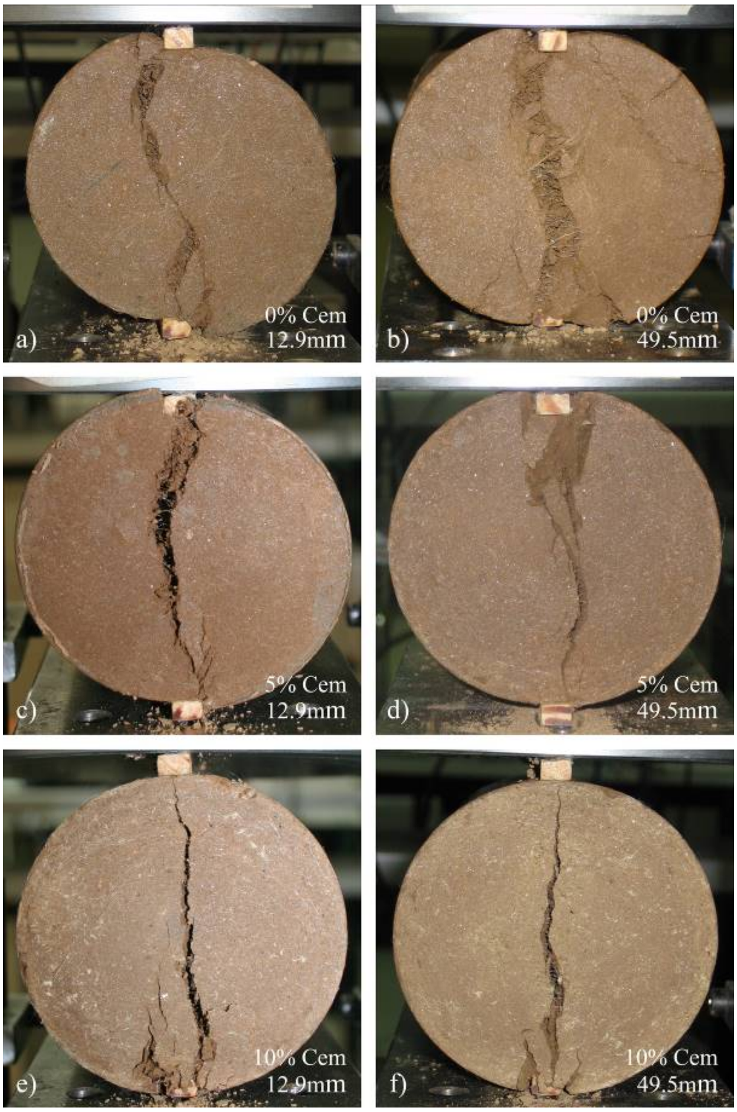

Figure 8: Failure mode of 0.20% fibre content specimens as a function of cement content and fibre length

The load *F* uniformly applied on two diametrically opposite generatrices of the cylindrical specimens produces a biaxial stress state, which is fully characterized by the elasticity theory (Carmona and Aguado, 2012). The vertical and horizontal stresses produced at the axis of the cylinder can be estimated using equations (1) and (2), respectively, based on the geometry – length (H) and diameter (D) – of the specimen. The maximum indirect tensile strength (peak horizontal stress) corresponding to each curve, which in BSi EN 13286 (2003) is designated by R_{it}, was calculated and the average values are presented in Figure 9.

$$\sigma_{hor} = R_{it} = \frac{2F}{\pi HD} \quad (1)$$

$$\sigma_{ver} = \frac{6F}{\pi HD} \quad (2)$$

It is again possible to conclude that the tensile strength increased with cement and fibre content, as well as fibre length. Additionally, the influence of fibre content on the R_{it} value was more significant on the mixtures with higher cement content, which might be explained by the increased adhesion between the fibres and the soil matrix, provided by the cement paste, i.e. the fibre influence on the overall behaviour depends on the adhesion with the soil particles, and the cement provide an efficient binding media that potentiates this adhesion. On the contrary, the mixtures with lower cement content will possess lower levels of chemical adhesion between the soil particles and the fibres, and thus the pull-out mechanism will rely mostly on the friction between the two materials. Another possible explanation could be the decrease in the voids ratio with the increase in fibre content. Such reduction in the proportion between the air and the solids creates more compacted specimens, which could influence the gripping of the soil particles over the fibres. However, although the reduction rate in the voids ratio was very similar along each cement content, the 10% cement specimens were clearly more affected by the fibre content than the 0% and 5% cement content specimens, which suggests that the binder improved the bonding between the particles and the fibres.

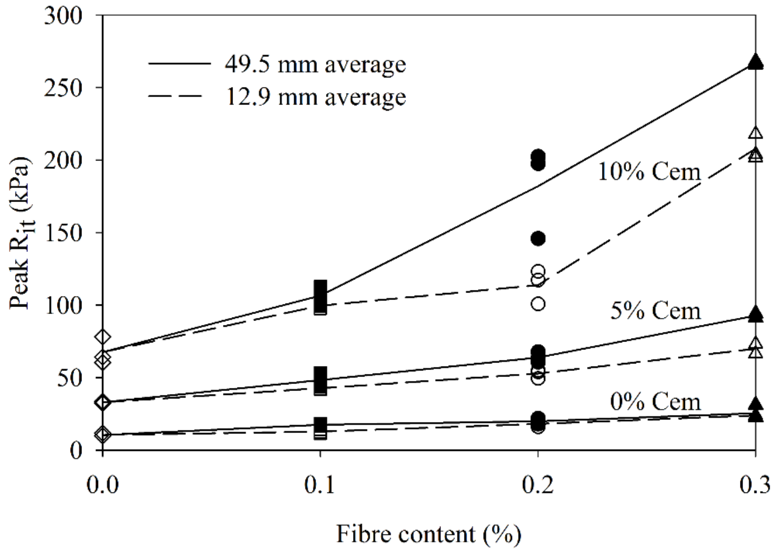

Figure 9: Average R_{it} at peak as a function of fibre and cement content

The stress applied on the vertical direction (plane formed by the opposite generatrices where the load is applied) was in turn estimated using Equation (2), and the average results were used to calculate the average secant modulus of each mixture (computed at 50% of the peak load). The results are presented in Figure 10, showing that both fibre length and content were influential on the pre-peak response of the 5 and 10% cementation levels.

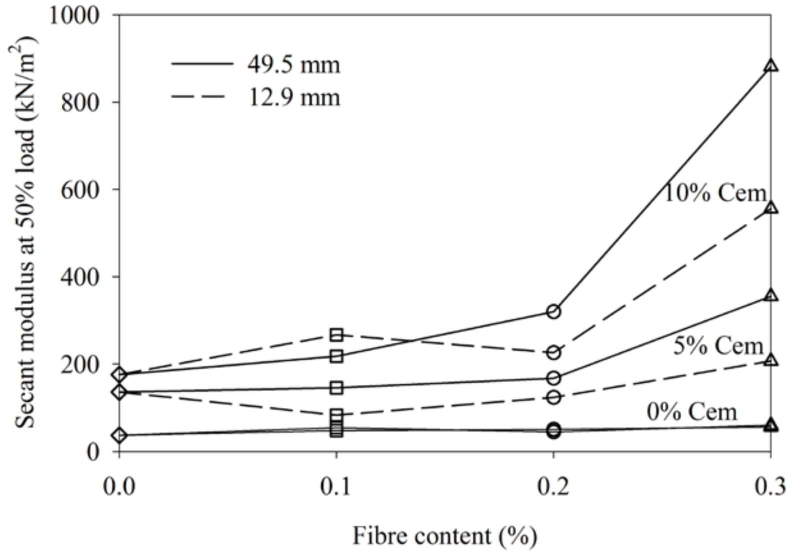

Figure 10: Secant modulus, obtained at 50% of the max load, as a function of cement, fibre content and fibre length

3.3. Triaxial compression behaviour

The triaxial tests results presented in Figure 11. The specimens prepared only with cement (10%, TA.2.0) and no fibres showed an increase in peak stress, relatively to the unreinforced specimens (TA.0.0). However, the post-peak behaviour is clearly more fragile. In turn, the specimens reinforced only with fibres (0.2%, TC.0.2) presented a smaller peak stress increase, as observed by Yetimoglu and Salbas (2003), but have shown an improvement on the post-peak response – in the case of the test with a confinement pressure of 50 kPa, a slightly strain-hardening behaviour was even observed.

It is interesting to compare this somehow small peak strength increase between unreinforced and fibre-reinforced (no-cement) specimens with the significant peak stress increase that was obtained, for similar specimens, in indirect tensile strength tests. This is in accordance with the results obtained by Ibraim et al. (2012), which concluded that moist tamping specimen preparation (which is, in concept, similar to the specimen preparation used in the present work) produced greater resistance to tensile strains in the horizontal direction. In compression triaxial tests this a fairly influential aspect, as demonstrated by the higher strength obtained with the fibre reinforced specimens, when compared with the unreinforced specimens (although less significant, it was clear). However, it is normal to expect that, in tensile-based applications, like the indirect tensile tests performed, the horizontal fibre orientation becomes even more relevant, which explains the more significant role that the fibres have played. The combination of the reinforcement and the chemical stabiliser proved to be very effective. These results can be interpreted in the following manner: adding a relatively small quantity of 49.5 mm fibres to an artificially cement soil increased its stiffness and more than doubled the peak stress.

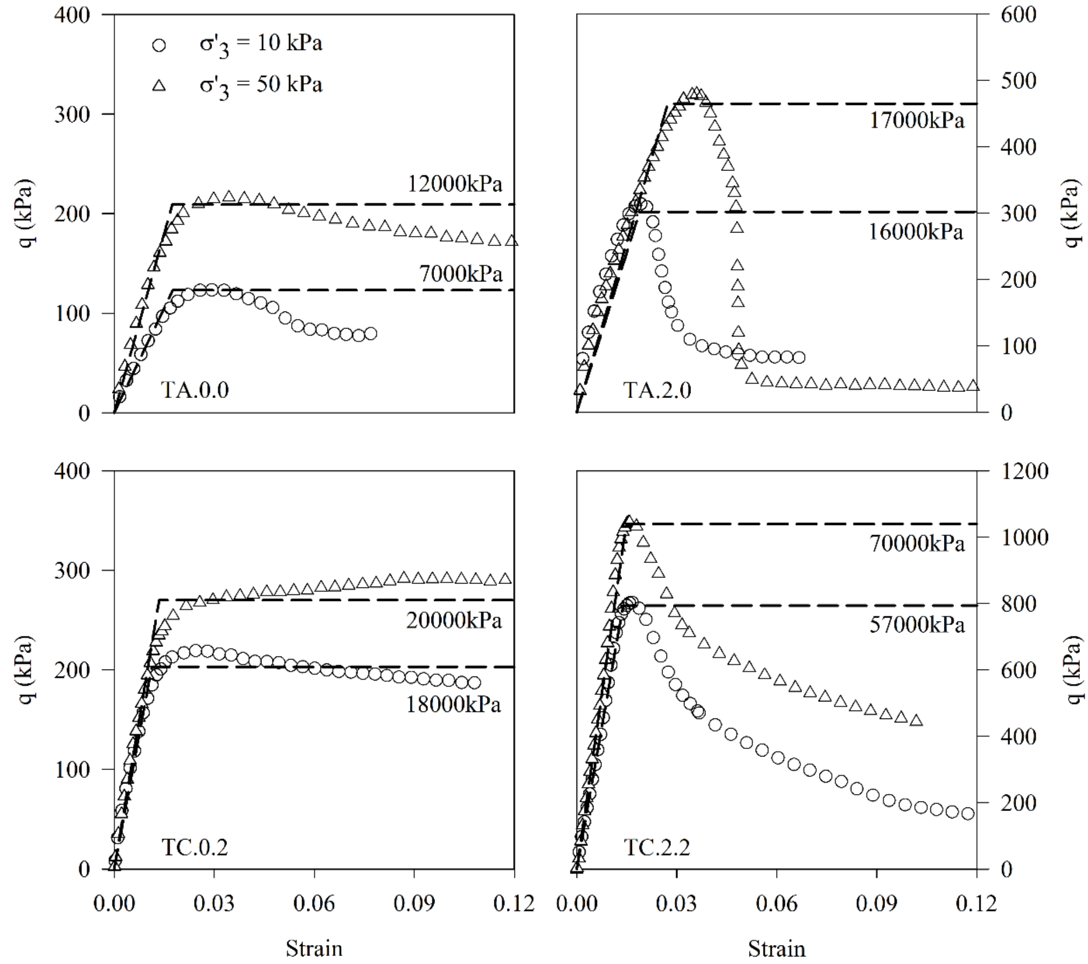

Figure 11: Triaxial compression tests performed on the original soil (TA.0.0), and on the soil stabilised with cement (TA.2.0) and reinforced with fibres (TC.0.2) and fibres+cement (TC.2.2). The Mohr-Coulomb failure criterion adjustment to the stress-strain curves is also presented

The Mohr-Coulomb constitutive criterion (MC) was used to model the stress-strain curves, up to the peak load, in elastoplastic constitutive conditions. The elastic-perfectly-plastic behaviour assumed by such model does not properly reproduce the post-peak strain-softening, registered during the plastic flow phase of most tests. However, the MC model implemented through Equation (3) allowed the retrieving of the yield value F. The model fit is shown graphically in Figure 11, and the retrieved values are presented in Table 3.

$$F(p',q) = q - \frac{6 \cdot sin\phi'}{3 - sin\phi'} \cdot p' - \frac{6 \cdot c' \cdot cos\phi'}{3 - sin\phi'} \qquad (3)$$

Cristelo N et al., Influence of fibre reinforcement on the post-cracking behaviour of a cement-stabilised sandy-clay subjected to indirect tensile stress, *Construction and Building Materials, Elsevier*, 138: 163-173, 2017.
Doi: 10.1016/j.conbuildmat.2017.02.010

Table 3
Backfill properties inferred from the adjustment of the Mohr-Coulomb constitutive model to the triaxial tests

Mixture ID	Mixture type	σ'_3 (kPa)	c' (kPa)	ϕ' (º)	E_{50} (kPa)
TA.0.0 (a)	Soil	10	30	32	7000
TA.0.0 (b)		50	30	32	12000
TA.2.0 (a)	Cem	10	60	43	16000
TA.2.0 (b)		50	60	43	17000
TC.0.2 (a)	Fibres	10	59	28	18000
TC.0.2 (b)		50	59	28	20000
TC.2.2 (a)	Cem +	10	137	49	57000
TC.2.2 (b)	fibres	50	137	49	70000

The internal peak friction angle (ϕ') increased from 32 to 43º with 10% cement, while an even more significant increase was registered for the cohesion (30 to 60 kPa). The addition of fibres (and no cement) produced an increase in strength, although with a slight decrease of the internal friction angle. The cohesion increase between the original soil and the fibre reinforced mixture was similar to that obtained between the soil and the soil-cement mixture, which is in accordance with the short peak-strength increase revealed by the triaxial tests. It is interesting to note that, contrary to the no-cement specimens, the addition of the same amount of fibres to a highly cemented matrix (10% cement, TC.2.2) produced a significant ϕ' increase (43 to 49º), as well as more than doubled the cohesion value (60 to 137 kPa). This corroborates the previous conclusions regarding the indirect tensile tests, i.e. the effect of fibre content is more visible with the increase of cementation.

4. Discussion

4.1. Failure criterion of the fibres

Li and Zornberg (2013) have proposed, for situations where the failure is governed by yielding of the fibres, the use of Equation (4) to estimate the maximum distributed tension induced by the fibres (t_t):

$$t_t = \chi \cdot \sigma_{f,ult} \tag{4}$$

where χ is the volumetric fibre content, defined as the ratio of the fibre volume over the volume of the soil-cement-fibre mixture; and $\sigma_{f,ult}$ is the ultimate tensile strength of an individual fibre, which was shown in Figure 6 to be approximately 426 MPa. Based on fibre density (8.92 kN/m^3) and dry unit weight of the specimens (18 kN/m^3), the maximum tension values for each specimen can be estimated as a function of the fibre content (Table 4).

Table 4
Maximum distributed tension on the available fibres, as determined by Eq. (4)

Fibre content (%)	χ	t_t (kPa)
0.1	0.00198	843
0.2	0.00359	1682
0.3	0.00592	2522

It is then possible to conclude that the t_t values are higher than the maximum R_{it} presented in Figure 9, meaning that the composite material is not taking full advantage of the tensile strength of the fibres. Such behaviour could be partially explained by several facts, such as the fact that not all fibres are oriented in the same direction; or the fact that they are not pulled at their full capacity at the exact same time. However, the difference between R_{it} and t_t is so significant that the most viable explanation is the fact that the fibres are not reaching their full strain capacity during the indirect tensile tests, and thus their yielding stress. Since the tensile behaviour of these fibres is temperature-dependent, different strains could be needed to achieve the yielding stress, depending on the temperature at the time of each test. However, both types of tests (tensile tests on the fibres and indirect tensile tests on the cylindrical specimens) were performed in the same room, with only a few weeks apart, and thus it is reasonable to assume very similar temperatures in both cases (the temperature measured during the fibre tensile tests was approximately 22.5ºC). Instead, the different strains are very likely originated by relative displacements (slip) between the particles and the surrounding soil particles, which enables the conclusion that fibre pull-out was the governing failure mode.

Table 5 presents the average R_{it} values, estimated using Equation (1), of the 49.5 mm specimens at 3, 4 and 5 mm of diametric displacement, while Figure 12 represents the ratio between the average R_{it} and the corresponding maximum t_t value, for each of the mentioned diametric displacements. It is interesting to note that the mobilised tensile stress, at each diametric displacement, increases with cement content (Figure 12a). Also, the rate at which the R_{it} / t_t ratio decreases with the diametric displacement (crack widening) (Figure 12b), is significantly higher for the 10% cement mixtures than the 5% and, especially, the 0% cement mixtures. Both effects are probably a consequence of the already mentioned superior bonding between the 10% cement matrix and the fibres (mitigating the governing pull-out failure mode), as well as its higher stiffness relatively to the 0% and 5% cement specimens. The superior bonding and increased stiffness diminishes the possibility of both ends of each fibre to strain as the crack widens, which becomes possible only for the exposed central segment. Thus, at lower diametric strains (3 mm), the less wide crack of the higher cementation mixtures has produced a lower number of yielded fibres. However, as the diametric strain evolves to 4 and 5 mm, the crack widening of the 10% cement specimens is more effective in forcing the fibres to reach their yield stress than the more ductile and less gripping 0% and 5% cement specimens.

One final relevant observation can be made based on Figure 12a, which is the decrease of the tensile strength efficiency with the increase of fibre content. This somehow unexpected result might be a consequence of the increased difficulty, with increased fibre content, in achieving adequate homogenisation. As a result, it is possible to conclude that the efficiency gains with increased fibre content are not linear, since a lower percentage of added fibres will actually be contributing to the tensile effort.

Table 5
Average R_{it} (kPa) obtained for the 49.5 mm specimens at selected values of diametric displacement

Cement content (%)	Fibre content (%)	Average R_{it} (kPa)		
		3 mm	4 mm	5 mm
0.0	0.1	17.5	16.4	15.9
	0.2	20.9	19.9	19.0
	0.3	23.1	22.5	21.6
5.0	0.1	44.1	40.7	37.5
	0.2	64.7	60.9	57.4
	0.3	86.9	80.2	72.6
10.0	0.1	74.0	58.4	51.7
	0.2	114.9	86.7	65.2
	0.3	135.1	93.5	78.1

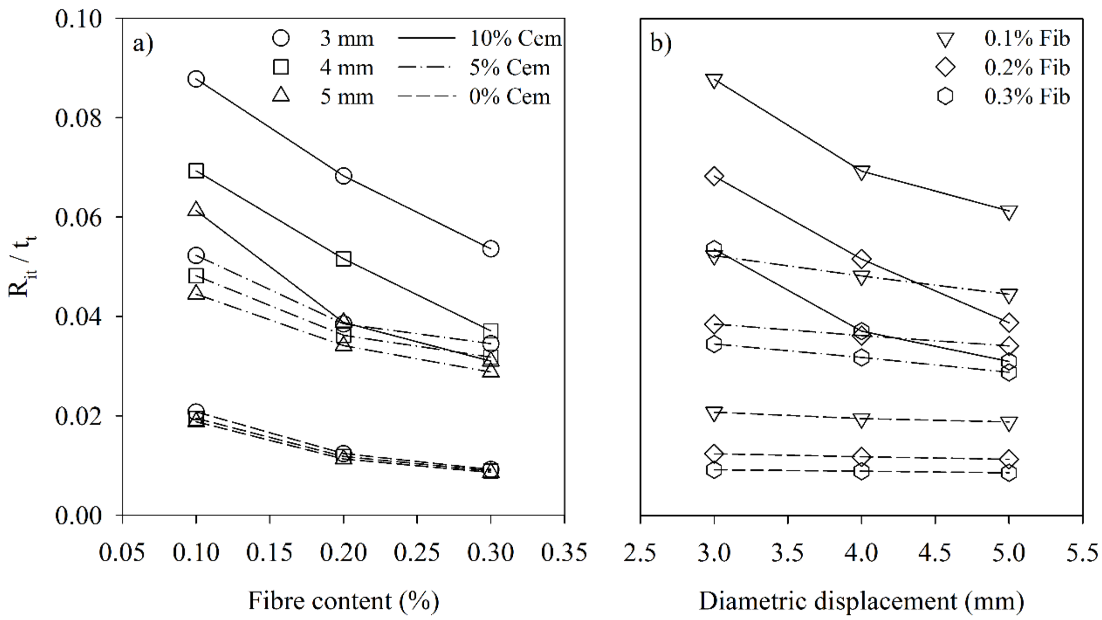

Figure 12: R_{it} / t_t ratio evolution of the 49.5 mm specimens as a function of fibre content (a) and diametric displacement (b)

4.2. Fibre content

Figure 13 shows that the correlation between the peak R_{it} and the corresponding diametric strain drastically decreases with the cementation level, corresponding to a decrease of the fibre content influence on the deformation at peak stress. This is a consequence of the fact that, without cement, all the fibres are included in the process of supporting the tensile forces, and thus the fibre content produces a high correlation between the R_{it} and the corresponding diametric strain. However, the addition of cement produces overall higher peak loads, for which some of the fibres are unable to resist, and thus a more random relation between R_{it} and diametric strain is attained.

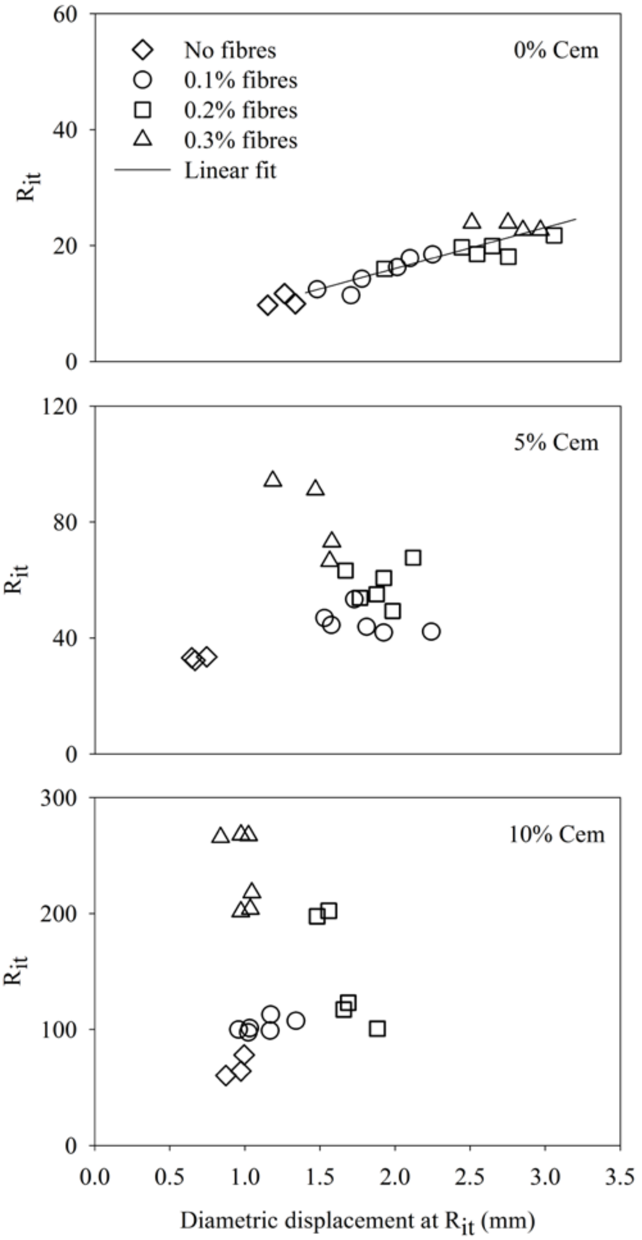

Figure 13: R_{it} as a function of diametric displacement, fibre content and cement content (note the different vertical scales)

4.3. Fibre length

In short, and based on Figure 8, it is possible to conclude that the peak load for the mixtures with the longer fibres is higher than that obtained with the 12.9 mm fibres. Also, for the 0.1% content, the post-peak strength loss rate of the 49.5 mm specimens was slower than the 12.9mm specimens, for every cement content. However, for the 0.2% and 0.3% fibre contents this is only true for the lower cement levels (0% and 5%). For the 10% cement content, the strength loss rate of the specimens with 49.5 mm was actually faster than the specimens with 12.9 mm. The aforementioned conclusions may be explained by the following consequences related to the cement content increase:

- First, the increase of the cement content will enhance the bond strength between the fibre / matrix. Therefore, up to the peak load, the chemical adhesion strength will be higher in the mixtures with higher cement content.
- The lengthier fibres have a higher aspect ratio, therefore for these mixtures, statistically speaking, there will be more fibres bridging an active crack contributing in a first stage to an increase of the peak load.
- The latter increase on the peak load will be more pronounced in the series with higher cement contents in which the interfacial bond strength is higher.
- In the post-peak behaviour, after the localization of the inelastic deformation and formation of the macro-crack, the energy release due to the fracture process of the matrix will be restrained by the fibres stitching the active crack. For the series with the lengthier fibres with higher peak loads, and consequently, higher energy accumulated, in particular for the series with 10% of cement, 0.20 and 0.30% of fibres, the developed frictional strength may lead to fibre rupture, and consequently to a sharper load decay in the softening stage.

4.4. Cement content

To better understand the relative influence of the cement and fibre content on the pre and post-peak response, the inclination of both segments (M_1 and M_2, respectively) was measured and the average M1 / M2 ratio was determined and presented in Figure 14. The secant modulus values, computed for 50% of the peak load as already presented in Figure 10, were used as the M1 values, while the M2 values correspond to the slope of the segment of the force-displacement curve indicated in Table 6.

The M1 / M2 ratio decrease between the 12.9 and 49.5 mm for the 10% cement mixtures, which is contrary to what happens with the 0 and 5% cement mixtures, translates the less relevant role of the fibres on the post peak behaviour of the matrix with the higher cement content. This idea is corroborated by the fact that the 10% cement M1 / M2 values are approximately constant with fibre length and content. The reason for this is that, although the higher fibre contents were responsible for the higher peak loads, they were not capable to bridge the higher stresses when the matrix started to fracture, i.e. an increase in fibre content produced higher peak-loads, but at the same time, led to a more accentuated load decay on the post-peak stage.

The same reasoning can be applied to the 0 and 5% cement content mixtures, in which the M1 / M2 ratios are significantly higher than those obtained for the 10% cement. For these lower cement contents, the fibres are able to bridge the stresses along the crack surfaces with a lower probability of fibre rupture. Within the 0% or the 5% cement results' sets, an increase in fibre content results in an increased M1 / M2 ratio, which is only possible (especially since there is a M1 increase) with a decrease of the M2 slope. It is important to remember that a M2 decrease means that the fibre's role becomes more influential.

In short, and based on Figure 10 and Figure 14, it is possible to conclude that the fibre content influence on pre-peak and post-peak response increases and decreases, respectively, as the soil matrix becomes more fragile (i.e. with the increase of the cement content of the soil matrix).

Cristelo N et al., Influence of fibre reinforcement on the post-cracking behaviour of a cement-stabilised sandy-clay subjected to indirect tensile stress, *Construction and Building Materials, Elsevier*, 138: 163-173, 2017.
Doi: 10.1016/j.conbuildmat.2017.02.010

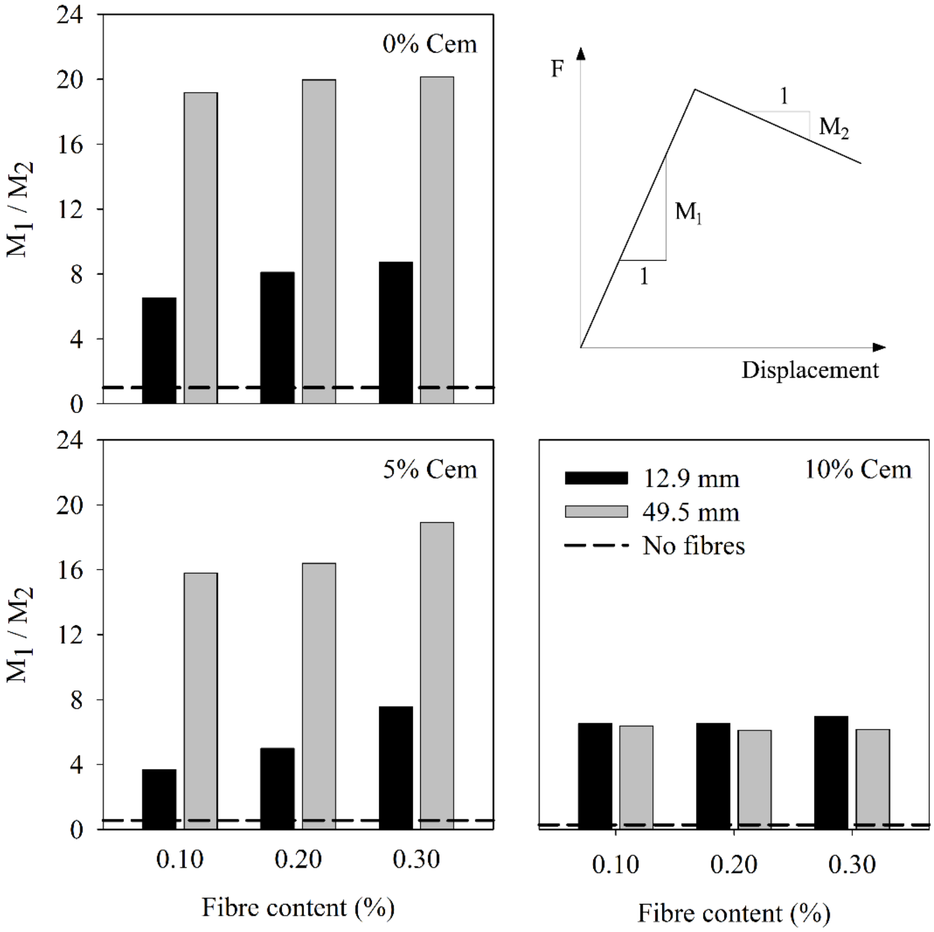

Figure 14: M1 / M2 slope ratio as a function of cement and fibre content

Table 6
Displacement intervals used to measure the M_2 inclinations

Cement content (%)	Fibre length (mm)	Minimum displacement (mm)	Maximum displacement (mm)
0.0	-	1.0	1.2
0.0	12.9	4.0	5.0
0.0	49.5	4.0	5.0
5.0	-	0.7	0.9
5.0	12.9	3.0	4.0
5.0	49.5	3.0	4.0
10.0	-	0.9	1.1
10.0	12.9	3.0	4.0
10.0	49.5	2.5	3.5

5. Conclusions

The indirect tensile strength of a fibre reinforced sandy-clay prepared with various fibre and cement contents was analysed and presented in this paper. Based on these results, the peak and especially the post-peak behaviour of the composite is better understood, with focus on the correlation between the fibre and cement content. The following main conclusions can be drawn:

- Pull-out was the governing failure mode.
- An increase in cement content reduces fibre influence on deformation.
- Fibre content influence on strain at peak stress decreases with increasing cementation.
- An increase in fibre content generates an increase in peak stress.
- Fibre content influence on pre and post-peak behaviour increases and decreases with cement content, respectively. As a consequence, the post-peak tension loss rate increases with fibre content.
- The mobilised post-peak stress does not increase linearly with fibre content, suggesting that homogenisation of the mixture is hindered by the increasing addition of fibres, and that a compromise must be found between peak and post-peak stress increase.
- Increase in fibre length results in increased peak stress, for every cement and fibre content, while fibre length influence on post-peak behaviour depends on fibre and cement content.
- If fibre reinforcement is intended, and thus the structure is expected to work beyond the ultimate limit state, a constitutive model more developed than the Mohr-Coulomb model is needed, in order to capture the post-peak residual behaviour of the composite material.

The addition of smaller quantities of reinforcement fibres, without artificial cementation and considering also the financial cost, can be considered as the most effective option, particularly when the application depends heavily on the tensile stress.

References

Al-Refeai, T.O., 1991. Behavior of granular soils reinforced with discrete randomly oriented inclusions. Geotext. Geomembranes 10, 319–333.

ASTM, 2011. D2487-11 Standard Practice for Classification of Soils for Engineering Purposes (Unified Soil Classification System).

BSi EN 13286, 2003. Unbound and hydraulically bound mixtures. Test method for the determination of the indirect tensile strength of hydraulically bound mixtures. Br. Stand. Institution, London.

Cai, Y., Shi, B., Ng, C.W.W., Tang, C.S., 2006. Effect of polypropylene fibre and lime admixture on engineering properties of clayey soil. Eng. Geol. 87, 230–240.

Carmona, S., Aguado, A., 2012. New model for the indirect determination of the tensile stress–strain curve of concrete by means of the Brazilian test. Mater. Struct. 45, 1473–1485.

Chauhan, M.S., Mittal, S., Mohanty, B., 2008. Performance evaluation of silty sand subgrade reinforced with fly ash and fibre. Geotext. Geomembranes 26, 429–435.

Consoli, N.C., Arcari Bassani, M.A., Festugato, L., 2010. Effect of fiber-reinforcement on the strength of cemented soils. Geotext. Geomembranes 28, 344–351.

Correia, A.A.S., Venda Oliveira, P.J., Custódio, D.G., 2015. Effect of polypropylene fibres on the compressive and tensile strength of a soft soil, artificially stabilised with binders. Geotext. Geomembranes 43, 97–106.

Cristelo, N., Cunha, V.M.C.F., Dias, M., Gomes, A.T., Miranda, T., Araújo, N., 2015. Influence of discrete fibre reinforcement on the uniaxial compression response and seismic wave velocity of a cement-stabilised sandy-clay. Geotext. Geomembranes 43, 1–13.

Diambra, A., Ibraim, E., Muir Wood, D., Russell, A.R., 2010. Fibre reinforced sands: Experiments and modelling. Geotext. Geomembranes 28, 238–250.

Eldesouky, H.M., Morsy, M.M., Mansour, M.F., 2013. Strength Parameters of Sand Reinforced with Randomly-Distributed Geosynthetic Fibers, in: G. Gottardi, Han, J., Ling, H., Tatsuoka, F., Cazzuffi, D. (Eds.), International Symposium on Design and Practice of Geosynthetic-Reinforced Soil Structures. DEStech Publications Inc., Bologna, pp. 63–72.

Falorca, I.M.C.F.G., Pinto, M.I.M., 2011. Effect of short, randomly distributed polypropylene microfibres on shear strength behaviour of soils. Geosynth. Int. 18, 2–11.

Gregory, G.H., 1998. Reinforced Slopes Using Geotextile-Fibers Composite, in: 30th Annual Southeastern Transportation Geotechnical Engineering Conference. FHWA, Louisville.

Gregory, G.H., 2011a. Sustainability aspects of the fiberreinforced soil repair of a roadway embankment, in: 24th Annual GRI Conference "Optimizing Sustainability Using Geosynthetics." Dallas.

Gregory, G.H., 2011b. Sustainability and the Fiber-reinforced Soil Repair of a Roadway Embankment. Geosynthetics 29, 18–22.

Gregory, G.H., Chill, D.S., 1998. Stabilization of Earth Slopes with Fiber Reinforcement, in: Rowe, R.K. (Ed.), Sixth International Conference on Geosynthetics. IGS, Atlanta, pp. 1073–1078.

Hamidi, A., Hooresfand, M., 2013. Effect of fiber reinforcement on triaxial shear behavior of cement treated sand. Geotext. Geomembranes 36, 1–9.

Ibraim, E., Diambra, A., Russell, A.R., Muir Wood, D., 2012. Assessment of laboratory sample preparation for fibre reinforced sands. Geotext. Geomembranes 34, 69–79.

Li, C., Zornberg, J., 2013. Mobilization of reinforcement forces in fiber-reinforced soil. J. Geotech. Geoenvironmental Eng. 139, 107–115.

Li, J., Tang, C., Wang, D., Pei, X., Shi, B., 2014. Effect of discrete fibre reinforcement on soil tensile strength. J. Rock Mech. Geotech. Eng. 6, 133–137.

Lirer, S., Flora, A., Consoli, N.C., 2011. On the Strength of Fibre-reinforced Soils. Soils Found. 51, 601–609.

Michalowski, R.L., Čermák, J., 2003. Triaxial Compression of Sand Reinforced with Fibers. J. Geotech. Geoenvironmental Eng. 129, 125–136.

Nasr, A.M., 2014. Behavior of strip footing on fiber-reinforced cemented sand adjacent to sheet pile wall. Geotext. Geomembranes 42, 599–610.

Olgun, M., 2013. Effects of polypropylene fiber inclusion on the strength and volume change characteristics of cement-fly ash stabilized clay soil. Geosynth. Int. 20, 263–275.

Sobhan, K., Mashnad, M., 2002. Tensile Strength and Toughness of Soil–Cement–Fly-Ash Composite Reinforced with Recycled High-Density Polyethylene Strips. J. Mater. Civ. Eng. 14, 177–184.

Tang, C., Shi, B., Gao, W., Chen, F., Cai, Y., 2007. Strength and mechanical behavior of short polypropylene fiber reinforced and cement stabilized clayey soil. Geotext. Geomembranes 25, 194–202.

Tang, C.-S., Shi, B., Zhao, L.-Z., 2010. Interfacial shear strength of fiber reinforced soil. Geotext. Geomembranes 28, 54–62.

Yetimoglu, T., Salbas, O., 2003. A study on shear strength of sands reinforced with randomly distributed discrete fibers. Geotext. Geomembranes 21, 103–110.

Yi, X.W., Ma, G.W., Fourie, A., 2015. Compressive behaviour of fibre-reinforced cemented paste backfill. Geotext. Geomembranes 43, 207–215.

Yilmaz, Y., 2015. Compaction and strength characteristics of fly ash and fiber amended clayey soil.

Eng. Geol. 188, 168–177.

Zhang, T., Liu, S., Cai, G., Puppala, A.J., 2015. Experimental investigation of thermal and mechanical properties of lignin treated silt. Eng. Geol. 196, 1–11.

Zhu, H.-H., Zhang, C.-C., Tang, C.-S., Shi, B., Wang, B.-J., 2014. Modeling the pullout behavior of short fiber in reinforced soil. Geotext. Geomembranes 42, 329–338.